MPMI Vol. 37, No. 2, 2024, pp. 84–92, https://doi.org/10.1094/MPMI-05-23-0052-TA

TECHNICAL ADVANCE

Assaying Effector Cell-to-Cell Mobility in Plant Tissues Identifies Hypermobility and Indirect Manipulation of Plasmodesmata

Mina Ohtsu,[1] Joanna Jennings,[1] Matthew Johnston,[1] Andrew Breakspear,[1] Xiaokun Liu,[1] Kara Stark,[1] Richard J. Morris,[2] Jeroen de Keijzer,[1] and Christine Faulkner[1,†]

[1] Cell and Developmental Biology, John Innes Centre, Norwich Research Park, U.K.
[2] Computational and Systems Biology, John Innes Centre, Norwich Research Park, U.K.

Accepted for publication 6 November 2023.

In plants, plasmodesmata establish cytoplasmic continuity between cells to allow for communication and resource exchange across the cell wall. While plant pathogens use plasmodesmata as a pathway for both molecular and physical invasion, the benefits of molecular invasion (cell-to-cell movement of pathogen effectors) are poorly understood. To establish a methodology for identification and characterization of the cell-to-cell mobility of effectors, we performed a quantitative live imaging-based screen of candidate effectors of the fungal pathogen *Colletotrichum higginsianum*. We predicted *C. higginsianum* effectors by their expression profiles, the presence of a secretion signal, and their predicted and in planta localization when fused to green fluorescent protein. We assayed for cell-to-cell mobility of nucleocytosolic effectors and identified 14 that are cell-to-cell mobile. We identified that three of these effectors are "hypermobile," showing cell-to-cell mobility greater than expected for a protein of that size. To explore the mechanism of hypermobility, we chose two hypermobile effectors and measured their impact on plasmodesmata function and found that even though they show no direct association with plasmodesmata, each increases the transport capacity of plasmodesmata. Thus, our methods for quantitative analysis of cell-to-cell mobility of candidate microbe-derived effectors, or any suite of host proteins, can identify cell-to-cell hypermobility and offer greater understanding of how proteins affect plasmodesmal function and intercellular connectivity.

Keywords: fungal effectors, fungus–plant interactions, microscopy and imaging, plasmodesmata

Cell-to-cell communication is essential for multicellularity, and cells use a variety of mechanisms to exchange information and resources. Plant cells are surrounded by cell walls but have tunnel-like structures called plasmodesmata that cross the cell wall and directly connect the cytoplasm of adjacent cells to establish the symplast. Small molecules such as sugars, metabolites, and hormones can all move between cells through plasmodesmata (Cheval and Faulkner 2018; Liu and Chen 2018; Stahl and Simon 2013), driven by cytoplasmic advection and diffusion. Further, larger proteins can pass between cells via mechanisms that involve active components such as protein unfolding and refolding or possible intercellular trafficking motifs/domains (Chen et al. 2013, 2014; Kragler et al. 1998; Taoka et al. 2007; Xu et al. 2011).

The regulation of plasmodesmata is a critical component of plant–microbe interactions. Many plant immune responses are triggered by cell autonomous recognition of pathogen molecules, but we and others have shown that plasmodesmata dynamically respond to immune signals. We previously found that both fungal and bacterial molecules induce plasmodesmal closure in *Arabidopsis thaliana.* Chitin (from fungal cell walls) and flg22 (from bacterial flagellin) both trigger plasmodesmal closure, regulated by LYSM-CONTAINING GPI-ANCHORED PROTEIN 2 (LYM2) and CALMODULIN-LIKE 41, respectively (Faulkner et al. 2013; Xu et al. 2017). Observations that plasmodesmal function influences infection outcomes identify that plasmodesmal responses are key to ultimate defense success (Faulkner et al. 2013; Lee et al. 2011; Xu et al. 2017). This suggests two possibilities: plasmodesmal regulation is important

[†]Corresponding author: C. Faulkner; christine.faulkner@jic.ac.uk

M. Ohtsu and J. Jennings contributed equally to this work.

Author contributions: M.O., J.J., X.L., A.B., K.S., and J.d.K. generated materials and performed experiments; M.O., J.J., A.B., and M.J. analyzed data; C.F. and R.J.M. supervised personnel; C.F. managed the project; and M.O., J.J., and C.F. wrote the paper with support from all coauthors.

Current address for M. Ohtsu: Division of Biological Science, Nara Institute of Science and Technology, 8916-5 Takayama, Ikoma, Nara 630-0192, Japan.

Current address for X. Liu: Lushan Botanical Garden, Chinese Academy of Sciences, Jiujiang, Jiangxi, China.

Current address for K. Stark: Developmental and Stem Cell Biology, Duke University, Durham, North Carolina, U.S.A.

Current address for J. de Keijzer: Cluster Plant Developmental Biology, Wageningen University, Droevendaalsesteeg 1, 6708 PB, Wageningen, The Netherlands.

Funding: Research in the Faulkner lab is supported by the H2020 European Research Council (725459, "INTERCELLAR") and the Biotechnology and Biological Sciences Research Council (BBS/E/J/000PR9796). M. Ohtsu was supported by the Japan Society for the Promotion of Science, X. Liu was supported by a Marie-Curie Fellowship (749755, "HOPESEE") from the H2020 European Research Council, J. Jennings was supported by the Norwich Research Park Doctoral Training Programme from the Biotechnology and Biological Sciences Research Council, and M. Johnston was supported by the John Innes Foundation Rotation PhD Studentship.

e-Xtra: Supplementary material is available online.

The author(s) declare no conflict of interest.

for the execution of plant immune responses and/or it impairs infection mechanisms deployed by the invading pathogens. The latter implicates pathogen access to the symplast as a critical component of infection.

Plasmodesmata present a route by which microbes can access noninfected cells and tissues. Indeed, there are several examples of pathogens directly using plasmodesmata to facilitate their passage between host cells in a growing infection. The best understood examples of this are infections by viruses such as *Cucumber mosaic virus* and *Tobacco mosaic virus* (Heinlein and Epel 2004). As obligate parasitic pathogens that infect intracellularly, viruses actively target and modify plasmodesmata to translocate their genomes between cells to establish an infection. Interestingly, it has also been revealed that some hemi-biotrophic fungal pathogens, including the rice blast pathogen *Magnaporthe oryzae*, pass from cell to cell at plasmodesmal pitfields (Kankanala et al. 2007). These findings demonstrate that plant pathogens across different kingdoms have acquired the capacity to recognize and exploit plasmodesmata as sites of connection between cells to enable the spread of infection.

To manipulate host plant systems, plant pathogens secrete an arsenal of proteins, called effectors (Le Fevre et al. 2015; Toruño et al. 2016). Because plasmodesmata allow the spread of soluble molecules, soluble effectors that are delivered into host cells also have the potential to move between cells via plasmodesmata. Indeed, *M. oryzae* produces the PWL2 and BAS1 effectors, which can move into noninfected cells (Khang et al. 2010). This suggests that pathogens exploit plasmodesmata to access and manipulate noninfected cells ahead of the infection front. Further implicating the symplast in infection, the *Fusarium oxysporum* effector Six5 was found to enable cell-to-cell translocation of its co-transcribed effector Avr2 via plasmodesmata (Cao et al. 2018). Moreover, both the *Pseudomonas syringae* effector HopO1-1 and the *Phytophthora brassicae* effector RxLR3 target and modify plasmodesmata (Aung et al. 2020; Tomczynska et al. 2020).

It is not yet fully understood how a microbe manipulates host plasmodesmata, or what a microbe gains by accessing the host symplast. To establish methods to address these questions, we characterized the cell-to-cell mobility of candidate effectors from the hemi-biotrophic fungal pathogen *Colletotrichum higginsianum*. We used a quantitative, live imaging-based screen to identify candidate effectors that move from cell to cell in plant tissues and found effectors that are cell restricted (immobile), move cell to cell to a degree expected for a protein of that size (mobile), and move farther than expected (hypermobile). Within the hypermobile effectors, we characterized two effectors that increase plasmodesmal conductivity, consistent with enhanced mobility. These effectors have differential effects on host cell processes and do not target characterized plasmodesmal regulators, suggesting plasmodesmata and cell-to-cell mobility can be modified in as yet undescribed ways. Our analysis shows that quantitative cell-to-cell mobility assays and linear modeling can reveal hypermobile protein behavior, correlated with an unexpected effect of cytosolic proteins on plasmodesmal function. While we have deployed this analysis to explore the behavior of non-endogenous proteins, these methods can be applied to endogenous proteins to reveal hypermobility across a range of signaling contexts.

Results

Identification of candidate cell-to-cell mobile *C. higginsianum* effectors

To establish a candidate list of putative *C. higginsianum* effectors (hereafter referred to as "effectors") exhibiting cell-to-cell mobility, we mined published transcriptomic data covering different infection stages (Dallery et al. 2017; O'Connell et al. 2012). Many effectors are secreted from pathogens into host plant tissues (Lo Presti et al. 2015), and therefore we limited our candidate cell-to-cell mobile effectors to those that encode conventionally secreted proteins with a predicted signal peptide. We also removed any sequences that had predicted transmembrane domains or glycosylphosphatidylinositol (GPI) anchors. Gene expression data in O'Connell et al. (2012) define expression profiles during the following stages of growth and infection: in vitro appressoria (VA), in planta appressoria (PA), biotrophic phase (BP) of infection, and necrotrophic phase (NP) of infection. We reasoned that cell-to-cell mobile effectors would be primarily relevant during the penetration (PA) and biotrophic phases (BP) of infection (i.e., when the host tissue is alive) and thus defined candidate cell-to-cell mobile effectors as those that have enhanced expression in PA and BP phases relative to the other two stages (i.e., PA/VA, BP/VA, PA/NP, and BP/NP > 2). We further arbitrarily limited candidates to those for which BP reads > 20 or PA > 50. After removing effectors with known domains that suggest they are unlikely to act as effectors, such as cell wall-modifying enzymes, our criteria produced a list of 33 candidates.

Plant proteins that are known to be cell-to-cell mobile are typically soluble within the cytoplasm or the nucleus (Chen et al. 2013; Gallagher and Benfey 2009; Gallagher et al. 2004; Kim et al. 2002), and we made the assumption that *C. higginsianum* cell-to-cell mobile proteins would have similar properties. Thus, to further refine our list of candidate cell-to-cell mobile effectors, we cloned these 33 candidate effectors as fusions to green fluorescent protein (GFP) and screened for nucleocytoplasmic and nuclear subcellular localizations by transient transformation of *Nicotiana benthamiana*. Of these 33 effector–GFP fusions, 20 (Supplementary Table S1) showed nucleocytoplasmic localization with strong enough expression to perform a cell-to-cell mobility assay. None showed a specific nuclear localization.

Live cell screening for cell-to-cell mobility

To assay the cell-to-cell mobility of nucleocytoplasmic effectors, we performed a live cell imaging-based screen using transient transformation of single epidermal cells in *N. benthamiana*. For this we used Golden Gate modular cloning (Engler et al. 2008) to assemble effector–GFP fusions and a cell transformation marker in a single backbone as a dual-expression cassette vector (Reyes Caldas et al. 2022; Fig. 1A). For a cell transformation marker, we used dTomato fused to a nuclear localization sequence (NLS-dTomato), reasoning that the dimerization properties of dTomato would make a protein complex too large to move from cell to cell.

To confirm the utility of NLS-dTomato as a cell transformation marker, we generated constructs that express GFP or 2×GFP with NLS-dTomato (pICH4723.GFP.NLS-dTomato and pICH4723.2xGFP.NLS-dTomato, respectively). *Agrobacterium tumefaciens* infiltration of *N. benthamiana* leaves at a low OD_{600} demonstrated that both fluorophores were expressed in the single transformed cell. While GFP was frequently seen to move freely from the transformed cell, both NLS-dTomato and 2×GFP were mostly retained within the transformed cell (Fig. 1; Supplementary Fig. S1).

Cell-to-cell mobility via plasmodesmata is dependent upon the size of the molecule (Crawford and Zambryski 2001; Oparka et al. 1999). To determine the relationship between size and mobility in *N. benthamiana* leaves in more detail, we assayed the mobility of four proteins of different sizes: GFP (26 kilodaltons [kDa]), YFP_C-GFP (the 91 C-terminal amino acids of YFP fused to GFP, 37.2kDa), YFP_N-GFP (the 161 N-terminal amino acids of YFP fused to GFP, 45 kDa), and 2×GFP (52 kDa)

(Supplementary Fig. S1). We generated single cell transformation sites by low OD_{600} *A. tumefaciens* infiltration of *N. benthamiana* leaves and counted the number of cells that exhibited GFP surrounding a transformed cell for each construct (marked by NLS-dTomato) (Fig. 1). We fit a quasi-Poisson function, which makes minimal assumptions, through the data, obtaining a smooth fit through the data that allows for the infrequent mobility of the larger standard proteins (Supplementary Fig. S1). However, we point out that the data do not exclude the existence of a size exclusion limit, which could be anywhere upward of 2×GFP. This model, with a Bonferroni-corrected confidence interval of the mean ($P < 1 \times 10^{-5}$), defined a standard curve against which to compare mobility of effectors of varying sizes.

Cell-to-cell mobility screen identifies mobile and hypermobile effectors

To characterize the cell-to-cell mobility of nucleocytoplasmic effectors, we cloned each of the 20 effectors in a dual-expression cassette vector as described (i.e., pICH4723.Effector-GFP.NLS-dTomato) (Fig. 1A). Assaying for cell-to-cell mobility, we observed varying degrees of cell-to-cell mobility for the effectors (Fig. 1B, bottom row); 6 effectors were restricted to the transformed cell (Fig. 1B, middle row) in *N. benthamiana* and 14 exhibited cell-to-cell mobility (Supplementary Fig. S2).

To determine whether an effector's mobility was as expected for a soluble protein of that size, we compared effector mobility with the standard curve (Fig. 2; Supplementary Fig. S1B). An exact Poisson test identified a subset of four effectors that had greater than expected mobility, and we defined these as "hypermobile" (Supplementary Fig. S3). To confirm that this hypermobility did not arise from cleavage of the effector–GFP fusion (to produce a smaller and thus more mobile protein), we assayed the protein size of the GFP-fused four hypermobile effectors expressed in *N. benthamiana* by protein extraction and Western blot analysis. Two strong bands for ChEC130-GFP were observed, suggesting this effector is cleaved in planta (Supplementary Fig. S4). However, the other three effectors showed little evidence

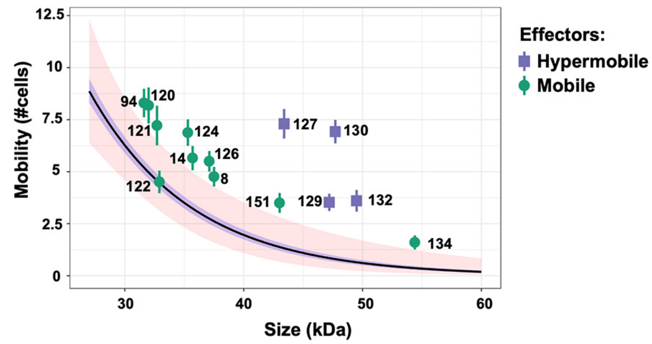

Fig. 2. Mobility quantification for nucleocytoplasmic effectors reveals mobile and hypermobile effectors. Mobility (number of cells to which green fluorescent protein [GFP] has moved around a transformed cell) of effector–GFP fusions. The standard curve is a quasi-Poisson generalized linear model with a log-link function and the Bonferroni-corrected confidence interval of the mean ($P < 1 \times 10^{-5}$) (pink shading). Effectors were determined to be significantly mobile (purple squares) by an exact Poisson test indicating the rate of movement is significantly different from the standard curve ($P < 1 \times 10^{-5}$). Data are means ± standard errors ($n > 30$, $P < 1 \times 10^{-5}$).

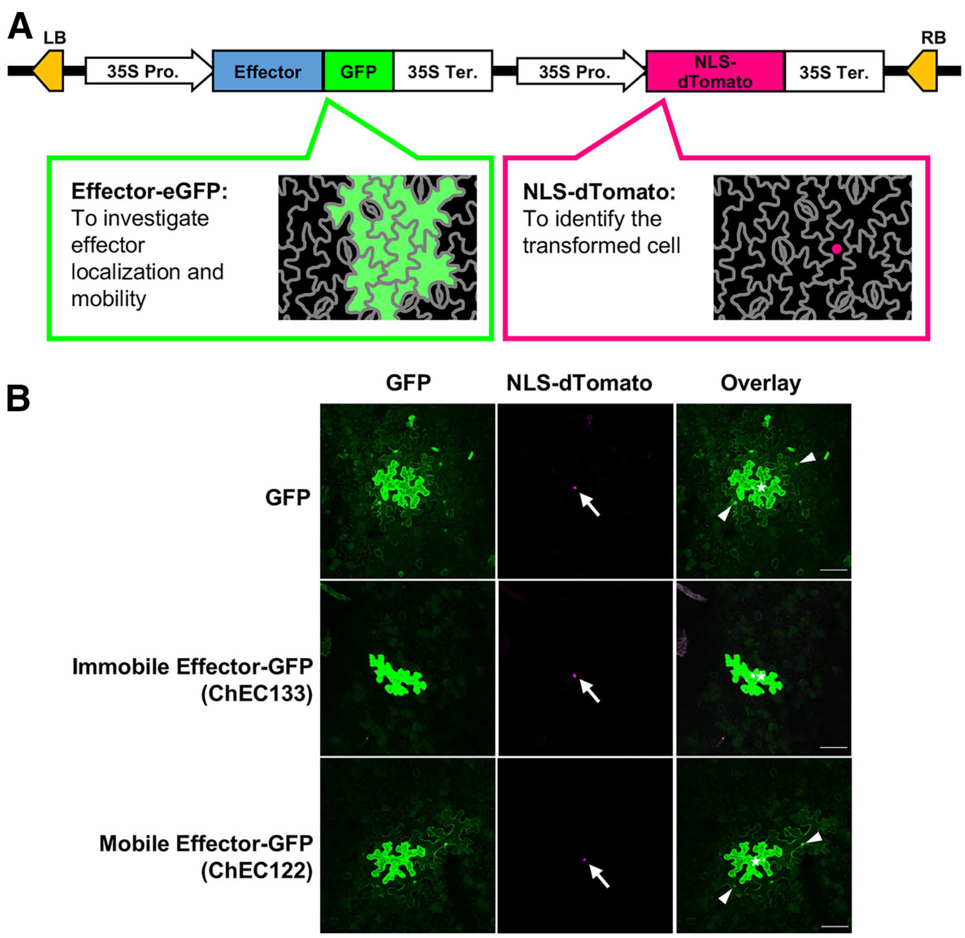

Fig. 1. Green fluorescent protein (GFP) fusions allow detection of cell-to-cell mobility screening of *Colletotrichum higginsianum* effectors. **A,** Schematic of the dual-expression module binary vectors used to screen for cell-to-cell mobility. The cartoon represents the patterns of localization for each module's gene product expected for a mobile effector–GFP fusion. **B,** Projections of confocal Z-stacks (8 to 20 individual focal planes, taken at 5.66-µm intervals) of tissues expressing GFP alone and effector–GFP fusions. Mobility is visible when cells surrounding the transformed cell, marked by NLS-dTomato, show GFP fluorescence. ChEC133-GFP (middle row) shows an example of a cell-restricted, immobile effector, while ChEC122-GFP (bottom row) shows an example of mobility to surrounding cells, as observed for GFP alone (top panel). Arrows indicate NLS-dTomato fluorescence in the transformed cell, asterisks (*) represent the transformed cells, and arrowheads represent cells the GFP has moved into. Scale bar: 100 µm.

of significant degradation or cleavage (Supplementary Fig. S4). Thus, we concluded that ChEC127, ChEC129, and ChEC132 are hypermobile.

Mobile effectors can modify plasmodesmal function

The identification of both mobile and hypermobile effectors suggests that *C. higginsianum* proteins might exploit and manipulate plasmodesmata via different mechanisms. Hypermobility suggests three possibilities: that the shapes, or Stokes radius, of such effectors allow for more efficient translocation through plasmodesmata; that effectors exploit an active translocation mechanism; or effectors modify plasmodesmata (directly or indirectly), which allows their passage. In this study, each of the effectors is fused to GFP, and therefore the Stokes radius of each fusion must be greater than that of GFP. Therefore, this is unlikely to be a significant factor in observed hypermobility. To address the question of whether mobile and hypermobile effectors modified plasmodesmal function, we exploited the unexpected low-level mobility of NLS-dTomato observed postcollection when the image contrast was adjusted (Supplementary Fig. S5). NLS-dTomato clearly marked the transformed cell in all cases, but when the contrast of the images was increased, it was additionally observed in an average of 2.5 surrounding cells in size-standard controls (Supplementary Figs. S5A and S6). We quantified NLS-dTomato movement when co-expressed with each mobile and hypermobile effector and observed variation in the spread of NLS-dTomato (Supplementary Figs. S5B and S6). To determine whether hypermobility is associated with a general increase in mobility that would indicate plasmodesmal regulation, we compared relative mobility of the effectors ($Mob_r = Mob_{obs}/Mob_{exp}$) to the mobility of NLS-dTomato when produced in the presence of the effector. If the effectors have no effect on plasmodesmal function, we would expect NLS-dTomato mobility to be constant across all effectors. Thus, we analyzed the data with an exact Poisson test, using the null hypothesis that mobility of NLS-dTomato is 2.5 cells for all values of Mob_r, and found that ChEC127 and ChEC8 both significantly increase NLS-dTomato mobility (Fig. 3A). This result suggests that ChEC127 and ChEC8 modify plasmodesmal function. Curiously, while ChEC127 is a hypermobile effector, ChEC8 is not, suggesting that despite modifying plasmodesmal function, the effector itself does not have increased translocation. This phenomenon might be explained if ChEC8 binds other proteins in plant cells to increase its effective size.

NLS-dTomato is targeted to the nucleus and therefore has a limited pool available in the cytoplasm for cell-to-cell movement. Further, NLS-dTomato is expected to dimerize to form a complex that we expect has reduced mobility as a consequence of increased size. Thus, this would render this protein a low-sensitivity marker for changes to plasmodesmal function, detecting only large changes to the plasmodesmal aperture. Therefore, we extended our analysis of plasmodesmal function in the presence of hypermobile mobile effectors to examine the mobility of cytoplasmic mRFP in *Arabidopsis*, a native host of *C. higginsianum*. For this, we generated *Arabidopsis* lines that stably express fluorescent protein fusions of the hypermobile effectors ChEC127 and ChEC132 (Supplementary Fig. S7)—ChEC127 has the highest Mob_r and ChEC132 is the largest hypermobile effector. We performed microprojectile bombardment assays (Tee et al. 2022) on expanded leaves of two independent transformed lines that express each effector and quantified spread of mRFP from transformed cells 1 day post-bombardment. These

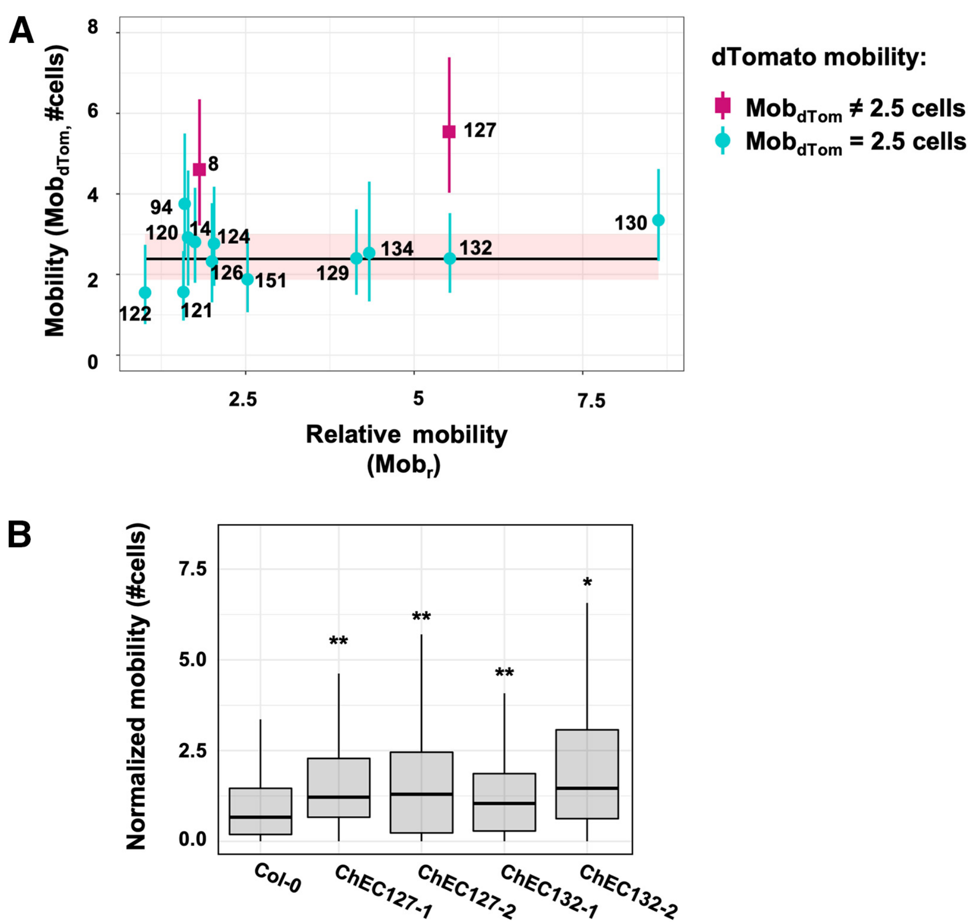

Fig. 3. Plasmodesmal regulation by mobile and hypermobile effectors. **A,** Mobility of NLS-dTomato plotted against the relative mobility (Mob_r) of a co-expressed effector in *Nicotiana benthamiana* leaf epidermal cells. The standard curve represents NLS-dTomato mobility in the presence of green fluorescent protein (GFP) variants of different sizes with Bonferroni-corrected confidence interval of the mean ($P < 1 \times 10^{-5}$) (pink shading). NLS-dTomato movement was analyzed by an exact Poisson test, identifying that ChEC8 and ChEC127 increase NLS-dTomato mobility. **B,** Mobility of mRFP (number of cells) in *Arabidopsis* leaf tissue assayed by microprojectile bombardment assays. Independent transgenic lines expressing ChEC127-GFP and ChEC132-GFP showed increased mobility of monomeric red fluorescent protein (mRFP) relative to Col-0. Boxes signify the upper and lower quartiles, and the whiskers represent the minimum and maximum within 1.5× interquartile range. The number of bombardment sites (n) counted is ≥92. Data were analyzed by bootstrap analysis, and asterisks (*) indicate statistical significance compared with Col-0 plants (**$P < 0.01$; *$P < 0.05$).

data showed that both ChEC127- and ChEC132-expressing lines showed increased movement of mRFP relative to the Col-0 control (Fig. 3B). This increase in plasmodesmal flux of GFP was not associated with a reduction in the amount of callose at plasmodesmata (Supplementary Fig. S8), quantified by live-imaging of aniline blue-stained callose. Thus, these data indicate that ChEC132 also modifies plasmodesmal function like ChEC127 and ChEC8, but that this might occur via a callose-independent mechanism.

Hypermobile effectors indirectly modify plasmodesmal function

The observation that effectors ChEC127 and ChEC132 modify the mobility of mRFP through plasmodesmata suggests that these effectors target plasmodesmal function. We initially screened effectors for nucleocytosolic localization, but to confirm that these effectors are not associated with plasmodesmata, we stained plasmodesmal callose with aniline blue in *Arabidopsis* tissue expressing ChEC127-GFP or ChEC132-GFP (Fig. 4A). Neither of the effectors showed colocalization with plasmodesmal callose, suggesting that they do not act directly on plasmodesmata.

Plasmodesmal function can be modified in response to a variety of stress conditions by signaling molecules such as calcium ions (Holdaway-Clarke et al. 2000) and reactive oxygen species (Rutschow et al. 2011). To explore which processes are perturbed in effector-expressing tissue to induce changes in plasmodesmal function, and to begin to explore what processes cell-to-cell mobile effectors might manipulate during infection, we performed transcriptomic RNA sequencing (RNA-Seq) analysis. Thus, we assayed changes to the plant transcriptome induced in plants constitutively expressing ChEC127-GFP and ChEC132-GFP relative to Col-0. We defined differentially expressed genes as those for which we detected at least a twofold up- or downregulation ($|\log_2[\text{fold change}]| \geq 1$) and a false discovery rate (FDR)-corrected P value < 0.01, and used GO Term Finder (Boyle et al. 2004) to identify biological processes that are significantly enriched within the differentially expressed genes for each effector.

Despite having a significant effect on plasmodesmal function, ChEC127 differentially regulated the expression of only 13 genes (11 upregulated and 2 downregulated; Supplementary Table S3). By contrast, expression of ChEC132 caused differential expression of 217 genes (36 upregulated and 181 downregulated; Supplementary Table S4). GO term analysis indicates constitutive expression of ChEC132-induced downregulation of genes associated with iron transport and responses, in addition to cell wall modification, growth, syncytium formation (5 *EXPANSIN* genes also represented in the cell wall-loosening GO term), and lipid metabolism (Fig. 4B). These data suggest that ChEC132 perturbs a variety of processes, several of which might perturb plasmodesmal function by yet uncharacterized processes.

Heterologous expression of ChEC127 promotes virulence

Pathogen effectors are assumed to positively regulate virulence, facilitating infection success. To assess whether the

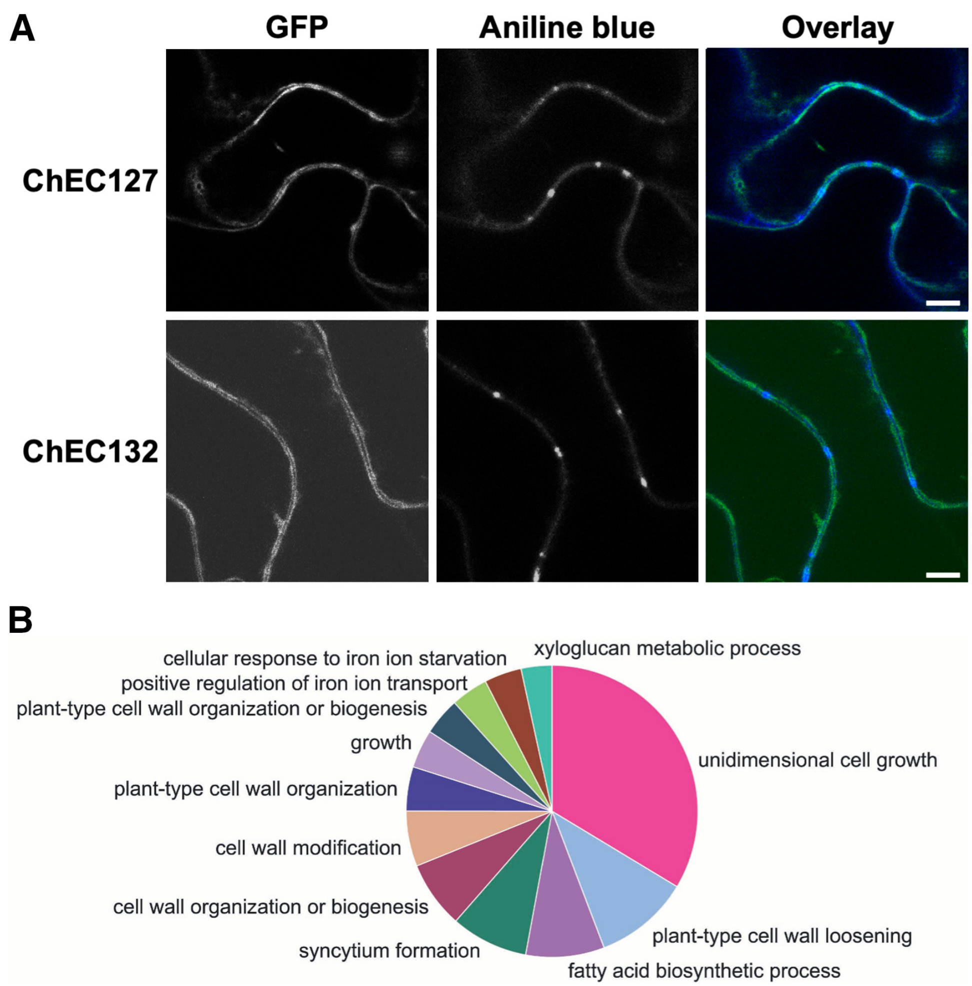

Fig. 4. Hypermobile effectors do not target plasmodesmata or alter host plant gene expression patterns known to be associated with cell-to-cell mobility or plasmodesmata. **A,** Confocal micrographs of *Arabidopsis* tissue expressing *Effector-GFP* (green fluorescent protein; left, green in overlay) stained with aniline blue (middle, blue in overlay) to mark plasmodesmata-associated callose. The right panel shows the overlay image. Scale bar: 10 µm. **B,** CirGO visualization of GO terms enriched among B genes downregulated by ChEC132. Slice size represents the proportion of differentially expressed genes (DEGs) attributed to this GO term.

hypermobile effectors ChEC127 and ChEC132 independently promote virulence, we infected plants constitutively expressing these effectors with *C. higginsianum* and measured the size of disease lesions 6 days postinoculation. These assays showed that both independent transgenic lines that express ChEC127 develop larger disease lesions (Fig. 5), identifying that expression of ChEC127 promotes virulence. Plants expressing ChEC132 showed no increase in susceptibility (Fig. 5), suggesting that this effector does not independently promote virulence under these conditions. Curiously, the effects of ChEC127 and ChEC132 on virulence are reversed relative to the effects on the host transcriptome.

Discussion

Host cell-to-cell connectivity is increasingly identified as a component of plant immunity and pathogen infection. This suggests that pathogen access to noninfected cells is important for the infection strategies of a range of pathogens. Previous studies have identified that specific effectors move cell-to-cell in host tissues (Cao et al. 2018; Khang et al. 2010), and it was suggested that cell-to-cell mobility is a property common to many proteins within an effector repertoire (Li et al. 2021). To investigate this further, we established methods to screen candidate effectors for cell-to-cell mobility of effectors from the hemi-biotrophic pathogen *C. higginsianum*. We generated a list of putative secreted effectors from publicly available data and used live-cell imaging to identify a subset of 20 candidate effectors that have a nucleocytoplasmic localization similar to many known cell-to-cell mobile molecules. Our live cell imaging-based screen for cell-to-cell mobility and analysis identified that 74% of nucleocytosolic effectors are cell-to-cell mobile (14/19), with 16% (3/19) showing greater than expected mobility (hypermobility) (Fig. 2; Supplementary Fig. S2).

In addition to identifying that cell-to-cell mobility is possible for a range of effectors, as was also recently identified for *P. syringae* effectors (Li et al. 2021), our data suggest that mobile proteins can also indirectly regulate plasmodesmata. Our quantitative approach enabled us to characterize effectors as immobile, mobile, or hypermobile. We expect that mobile effectors move "passively"' from cell to cell, that is, they move through

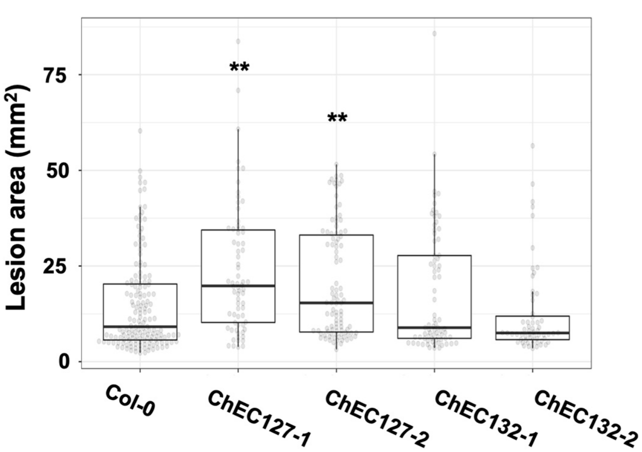

Fig. 5. *ChEC127*-expressing *Arabidopsis* are more susceptible to *Colletotrichum higginsianum*. Detached leaves from 4- to 5-week-old *Arabidopsis* plants were inoculated with *C. higginsianum* spores, and disease lesion areas were measured at 6 days postinoculation ($n > 60$). Boxes signify the upper and lower quartiles, whiskers represent the minimum and maximum within 1.5× interquartile range, and gray dots indicate individual data points. Bootstrap analysis of the lesion area means identified that lesions are larger in *ChEC127*-expressing plants (**$P < 0.01$).

plasmodesmata at a rate expected for soluble molecules of the same size (Fig. 2). Like the endogenous plant transcription factor LEAFY (Wu et al. 2003), these molecules can be considered to have no mechanism for active translocation and simply move from cell to cell as soluble, freely diffusive molecules. By analyzing two hypermobile effectors, ChEC127 and ChEC132, we found that hypermobile proteins can modify plasmodesmal function. These effectors trigger plasmodesmata opening to a degree such that the effector itself (Fig. 2), as well as other soluble molecules (as observed for mRFP; Fig. 3B), can move faster and farther to neighboring cells. Our analysis method has identified different mechanisms by which individual proteins regulate and access the symplast and would further identify proteins with an active mechanism of active translocation (i.e., are hypermobile but do not modify plasmodesmata). These mechanisms are likely to be represented in effector repertoires of different invasive microbes, as well as across endogenous soluble proteins.

Our data indicate that proteins interact with the symplast in different and complex ways, suggesting that a similar diversity of mechanisms of interaction with the symplast exists for soluble proteins across a wide range of contexts. The methods we used here, establishing a standard curve and using a linear model for analysis, allowed us to reveal not only cell-to-cell mobile behavior of the expected magnitude, but also hypermobile behavior. Many studies investigate the cell-to-cell mobility of individual proteins, but we and others are increasingly interested in the processes that are underpinned by cell-to-cell mobility and thus need to identify novel cell-to-cell mobile proteins. Most analyses are currently low resolution, grouping mobility greater than an arbitrary number of cells or cell layers in a single measure, relying on pairwise comparisons to a single control or with no comparison at all. Indeed, mobility is identifiable without a control, but our approach to collect quantitative and standardized data reveals more complex phenomena. Our strategy establishes a framework via which cell-to-cell mobile protein behavior can be more exhaustively dissected.

Our screen revealed that three nucleocytoplasmic effectors can modify plasmodesmal function (ChEC8, ChEC127, and ChEC132) despite not being associated with plasmodesmata. This raises biological questions relating to the different means by which microbial proteins interact with the host symplast during infection. Indeed, when we consider that it is likely that an effector cocktail simultaneously acts during infection to promote infection in host cells, we need to expand our hypotheses to encompass the effects on plasmodesmata from proteins that are not obvious plasmodesmal regulators (i.e., do not localize to plasmodesmata). That we identified multiple effectors that modify plasmodesmata during infection raises the possibility that there is a general increase in plasmodesmal aperture that might perturb multiple host and infection processes.

To identify host processes that might mediate effector-triggered changes to plasmodesmal function, we performed an RNA-Seq analysis of plants constitutively expressing the hypermobile effectors ChEC127 and ChEC132 (Supplementary Tables S3 and S4). This analysis presented contrasting transcriptional effects of these two hypermobile effectors: ChEC127 induced limited changes in the leaf transcriptome, while ChEC132 induced significant changes that indicate perturbation of a broad range of biological processes. While this analysis did not identify obvious targets via which effectors might impact plasmodesmata, ChEC127 upregulated expression of three genes described as encoding glycine-rich RNA-binding proteins (At1g7870, At5g45350, At4g38680) that have also been associated with plasmodesmal regulation and cell-to-cell mobility (Ueki and Citovsky 2005; Yan et al. 2020). ChEC132 induced downregulation of genes associated with fatty-acid metabolic processes, and it is well established that lipid composition of the plasmodesmal membrane affects plasmodesmal function (Grison et al. 2015) and thus is a possible mechanism by which ChEC132 indirectly modulates plasmodesmal function. That neither ChEC132 nor ChEC127 associates with plasmodesmata or regulates expression of known plasmodesmal regulators further demonstrates the potential of our approach to identify novel mechanisms of plasmodesmal regulation.

Live-cell imaging and quantitative analysis of the cell-to-cell mobility of *C. higginsianum* effectors has identified that this microbe produces candidate effectors that are both mobile and hypermobile in planta. For the effectors we further characterized, hypermobility was correlated with an indirect effect on plasmodesmal functional aperture, allowing an increase in nonspecific mobility between cells. These effectors are not associated with plasmodesmata or with the regulation of known plasmodesmal components, illustrating that plasmodesmata and the symplast are regulated by a variety of processes. These methods can be applied across a variety of systems to identify hypermobility of proteins and plasmodesmal regulation in novel contexts.

Materials and Methods

Plant material

N. benthamiana plants were grown at 23°C under long-day conditions (16 h:8 h, light/dark). *Arabidopsis thaliana* plants were grown on soil at 22°C under short-day conditions (10 h:14 h, light/dark) or on Murashige and Skoog medium under short-day conditions (10 h:14 h, light/dark).

DNA constructs

Constructs for plant expression were assembled using the Golden Gate cloning method (Engler et al. 2008); all module information is in Supplementary Table S2. The coding sequences of effector candidates (without predicted signal peptides) were domesticated to remove *Bpi*I and *Bsa*I sites and synthesized as Golden Gate-compatible Level 0 vectors. For subcellular localization analysis, effector sequences were fused to the N-terminus of GFP and expressed from the CaMV 35S promoter. For the cell-to-cell mobility assay and generation of *Arabidopsis* stable lines, multicomponent binary vectors were assembled as outlined in Supplementary Figure S1 and Supplementary Table S2.

Plant transformation

Transient gene expression in *N. benthamiana* was performed as previously described (Cheval et al. 2020). *A. tumefaciens* (GV3101) carrying binary plasmids was infiltrated into *N. benthamiana* leaves at $OD_{600nm} = 1.0 \times 10^{-2}$ to check subcellular localization and at $OD_{600nm} = 1.0 \times 10^{-5}$ to generate single-cell transformation events for the mobility assay. Samples were imaged 72-h postinfiltration. Stable transgenics were made by floral dipping *Arabidopsis* Col-0.

Microscopy

Abaxial leaf tissue was imaged by confocal microscopy (Zeiss LSM800) with a 20× water-dipping objective (W N-ACHROPLAN 20×/0.5; Zeiss). GFP was excited with a 488-nm solid-state laser and collected at 509 to 530 nm, and dTomato was excited by a 561-nm solid-state laser and collected at 600 to 640 nm using sequential scanning.

Image and data analysis

To quantify effector–GFP mobility, we recorded the number of fluorescent cells around the transformed cell, identified by NLS-dTomato fluorescence. Data analysis was performed in R statistical computing language v4.0.3 (R Core Team 2020). The standard curve was generated with data obtained from mobility of GFP, YFP_N-GFP, YFP_C-GFP, and 2×GFP using a quasi-Poisson generalized linear model with a log-link function and a Bonferroni-corrected P value $< 1 \times 10^{-5}$. Effectors were determined to be significantly mobile by the equivalent of a t-test for Poisson distributions (an exact Poisson test) in which the mobility (cell count at 3 days postinoculation) is significantly different to the standard curve ($P < 1 \times 10^{-5}$). For analysis of NLS-dTomato movement in the presence of different effectors, we tested the null hypothesis that mobility of NLS-dTomato is 2.5 cells (as observed for the set of standard constructs) and independent of effector mobility using an exact Poisson test.

Protein extraction and Western blotting

Protein extraction was performed as previously described (Adachi et al. 2019). *N. benthamiana* leaf tissue transiently expressing effectors was collected for protein extraction at 3 days postinfiltration. Leaf material was homogenized in ice-cold extraction buffer (10% glycerol, 25 mM Tris pH 7.5, 1 mM ethylenediaminetetraacetic acid, 150 mM NaCl, 2% wt/vol PVPP, 10 mM dithiothreitol, protease inhibitor cocktail [Sigma], 0.2% Igepal [Sigma]), and the soluble fraction was collected by centrifugation at 12,000 × g for 10 min. Proteins were separated by SDS-PAGE and transferred to PVDF membrane (Bio-Rad). Proteins were detected with 1/5,000-diluted anti-GFP conjugated to horseradish peroxidase (sc-9996; Santa Cruz Biotechnology).

C. *higginsianum* infection

C. higginsianum spores (5×10^6 spores/ml) were drop-inoculated on detached leaves of 4- to 5-week-old *Arabidopsis* plants on 2% water agar plates. Plates were sealed with parafilm and left for 6 days under short-day conditions (10 h:14 h, light/dark; 25°C). The area of necrotic lesions was measured in Fiji (Schindelin et al. 2012). Lesions were measured for at least 30 plants (2 leaves per plant) and across three independent experiments. The mean lesion area for different lines was compared using a bootstrapping method (Johnston and Faulkner 2021).

Microprojectile bombardment

Microprojectile bombardment assays were performed as previously described (Faulkner et al. 2013). Four- to six-week-old expanded leaves of relevant *Arabidopsis* lines were bombarded with 1-nm gold particles (Bio-Rad) coated with pB7WG2.0-mRFP, using a Biolostic PDS-1000/He particle delivery system (Bio-Rad). Bombardment sites were imaged at 24 h postbombardment by confocal microscopy (Zeiss LSM800) with a 10× (EC Plan-NEOFLUAR 10 × 0.3; Zeiss) or 20× dry objective (Plan-APOCHROMAT 20×/0.8; Zeiss). Data were collected from at least two independent bombardment events, each of which consisted of leaves from at least three individual plants. The median normalized mobility (no. of cells) for different lines was analyzed in R statistical computing language v4.0.3 (R Core Team 2020) by a bootstrap method (Johnston and Faulkner 2021).

Callose staining and quantification

Plasmodesmal callose was stained using a 1% (wt/vol) solution of aniline blue (415049; Sigma-Aldrich) dissolved in phosphate-buffered saline (pH 7.0). Briefly, mature leaves taken from 6-week-old, soil-grown *Arabidopsis* rosettes were infiltrated with aniline blue, washed in distilled water, and mounted on a microscope slide. Z-stacks of the lower epidermis were acquired at 1-μm intervals using a Zeiss LSM800 confocal microscope with a water immersion 63× objective lens (C Apochromat 63×/1.2 W Korr ultraviolet-visible-infrared water). Excitation of aniline blue was achieved using the 405-nm laser at 3.5% power, and the resulting signal was collected using a short-pass 470-nm filter. Images were acquired at 16-bit depth and 1,024 × 1,024 pixel resolution using 2× line averaging. Five leaves were imaged for each genotype, collecting 5 Z-stacks for each leaf (for a total of 25 Z-stacks per genotype).

Fiji was used to derive an average intensity projection from each Z-stack, and the elliptical selection tool was used to mask stomata and background signal. Plasmodesmal callose staining was quantified using a previously described Fiji macro (Bellandi et al. 2022; https://doi.org/10.5281/zenodo.6583765) with the following input parameters: threshold = 5,000, minsize = 5, and maxsize = 100. A statistical analysis of the resulting mean integrated density of detected particles per image for each genotype was conducted in R using Shapiro-Wilk and one-way analysis of variance tests.

Quantitative PCR (qPCR)

For comparison of transgene expression, *Arabidopsis* seedlings were grown in vitro on 1× Murashige and Skoog medium plus 1% sucrose for 14 days in long-day conditions (16 h:8 h light/dark, 22°C). Three seedlings were harvested per sample, and the experiment was performed in triplicate to provide three biological replicates. Harvested samples were snap frozen on liquid nitrogen and ground to a fine powder using a Geno Grinder (SPEX Sample Prep). RNA extraction, DNase treatment, first-strand cDNA synthesis, and qPCR were performed as previously described (Bellandi et al. 2022). Primers used to amplify short regions of ChEC127, ChEC132, and At*UBQ10* (housekeeping gene) are detailed in Supplementary Table S5. Normalized relative quantities (NRQs) were generated using the qBase model (Hellemans et al. 2007), and two-tailed *t*-tests for samples with unequal variances were used to test for significant differences in NRQs between transformants.

RNA-Seq analysis and GO term analyses

Leaves 7 and 8 of 4-week-old MS-grown *Arabidopsis* were harvested for RNA extraction. Leaves from three plants were pooled for a single replicate, and three replicates were collected for each genotype. RNA was extracted using RNAeasy Mini Kit (Qiagen) followed by DNase treatment (TurboDNase, ThermoFisher Scientific). Library preparation and Illumina sequencing (PE150, Q30 > 80%) with 10M paired reads was performed by Novogene. Sequencing reads quality was evaluated using FastQC v0.11.9 (Andrews 2010) and multiqc v1.9 (Ewels et al. 2016). After quality control, Trimmomatic v0.39 was used to remove Illumina sequence adapters and low-quality reads. Processed reads were reassessed with FastQC v0.11.9 and mapped to the *A. thaliana* TAIR10 release 37 genome assembly using hisat2 v2.2.0 and Samtools v1.11 (Li et al. 2009).

Differential expression analysis was performed with DESeq2 v1.20.0 (Love et al. 2014) and the R statistical computing language v4.0.3 (R Core Team 2020). Analysis methods described by Love et al. (2014) were used to calculate normalized expression values for each gene across all samples. Normalized expression values were compared for all expressed genes in Col-0 to those in the effector expressing lines using a hypergeometric test with the Benjamini and Hochberg FDR correction. Differentially expressed genes were defined by $|\log_2[\text{fold change}]| \geq 1$ and FDR-corrected P value < 0.01. Differentially expressed genes were analyzed by GoTermFinder (Boyle et al. 2004) with a hypergeometric test with a Bonferroni correction to identify biological processes enriched in the samples (adjusted P value $<$ 0.01). CirGO (Kuznetsova et al. 2019) was used to visualize the results.

Data statement

All raw data (images, RNA-Seq and quantification, and analysis of experimental data) will be made available in relevant public repositories or as Supplementary Material.

Literature Cited

Adachi, H., Contreras, M. P., Harant, A., Wu, C.-h., Derevnina, L., Sakai, T., Duggan, C., Moratto, E., Bozkurt, T. O., Maqbool, A., Win, J., and Kamoun, S. 2019. An N-terminal motif in NLR immune receptors is functionally conserved across distantly related plant species. eLife 8: e49956.

Andrews, S. 2010. FastQC: A quality control tool for high throughput sequence data. http://www.bioinformatics.babraham.ac.uk/projects/fastqc

Aung, K., Kim, P., Li, Z., Joe, A., Kvitko, B., Alfano, J. R., and He, S. Y. 2020. Pathogenic bacteria target plant plasmodesmata to colonize and invade surrounding tissues. Plant Cell 32:595-611.

Bellandi, A., Papp, D., Breakspear, A., Joyce, J., Johnston, M. G., de Keijzer, J., Raven, E. C., Ohtsu, M., Vincent, T. R., Miller, A. J., Sanders, D., Hogenhout, S. A., Morris, R. J., and Faulkner, C. 2022. Diffusion and bulk flow of amino acids mediate calcium waves in plants. Sci. Adv. 8:eabo6693.

Boyle, E. I., Weng, S., Gollub, J., Jin, H., Botstein, D., Cherry, J. M., and Sherlock, G. 2004. GO::TermFinder—open source software for accessing Gene Ontology information and finding significantly enriched Gene Ontology terms associated with a list of genes. Bioinformatics 20:3710-3715.

Cao, L., Blekemolen, M. C., Tintor, N., Cornelissen, B. J. C., and Takken, F. L. W. 2018. The *Fusarium oxysporum* Avr2-Six5 effector pair alters plasmodesmatal exclusion selectivity to facilitate cell-to-cell movement of Avr2. Mol. Plant 11:691-705.

Chen, H., Ahmad, M., Rim, Y., Lucas, W. J., and Kim, J.-Y. 2013. Evolutionary and molecular analysis of Dof transcription factors identified a conserved motif for intercellular protein trafficking. New Phytol. 198:1250-1260.

Chen, H., Jackson, D., and Kim, J.-Y. 2014. Identification of evolutionarily conserved amino acid residues in homeodomain of KNOX proteins for intercellular trafficking. Plant Signal Behav. 9:e28355.

Cheval, C., and Faulkner, C. 2018. Plasmodesmal regulation during plant-pathogen interactions. New Phytol. 217:62-67.

Cheval, C., Samwald, S., Johnston, M. G., de Keijzer, J., Breakspear, A., Liu, X., Bellandi, A., Kadota, Y., Zipfel, C., and Faulkner, C. 2020. Chitin perception in plasmodesmata characterizes submembrane immune-signaling specificity in plants. Proc. Natl. Acad. Sci. U.S.A. 117: 9621-9629.

Crawford, K. M., and Zambryski, P. C. 2001. Non-targeted and targeted protein movement through plasmodesmata in leaves in different developmental and physiological states. Plant Physiol. 125: 1802-1812.

Dallery, J.-F., Lapalu, N., Zampounis, A., Pigné, S., Luyten, I., Amselem, J., Wittenberg, A. H. J., Zhou, S., de Queiroz, M. V., Robin, G. P., Auger, A., Hainaut, M., Henrissat, B., Kim, K.-T., Lee, Y.-H., Lespinet, O., Schwartz, D. C., Thon, M. R., and O'Connell, R. J. 2017. Gapless genome assembly of *Colletotrichum higginsianum* reveals chromosome structure and association of transposable elements with secondary metabolite gene clusters. BMC Genomics 18:667.

Engler, C., Kandzia, R., and Marillonnet, S. 2008. A one pot, one step, precision cloning method with high throughput capability. PLoS One 3:e3647.

Ewels, P., Magnusson, M., Lundin, S., and Käller, M. 2016. MultiQC: Summarize analysis results for multiple tools and samples in a single report. Bioinformatics 32:3047-3048.

Faulkner, C., Petutschnig, E., Benitez-Alfonso, Y., Beck, M., Robatzek, S., Lipka, V., and Maule, A. J. 2013. LYM2-dependent chitin perception limits molecular flux via plasmodesmata. Proc. Natl. Acad. Sci. U.S.A. 110:9166-9170.

Gallagher, K. L., and Benfey, P. N. 2009. Both the conserved GRAS domain and nuclear localization are required for SHORT-ROOT movement. Plant J. 57:785-797.

Gallagher, K. L., Paquette, A. J., Nakajima, K., and Benfey, P. N. 2004. Mechanisms regulating SHORT-ROOT intercellular movement. Curr. Biol. 14:1847-1851.

Grison, M. S., Brocard, L., Fouillen, L., Nicolas, W., Wewer, V., Dörmann, P., Nacir, H., Benitez-Alfonso, Y., Claverol, S., Germain, V., Boutté, Y., Mongrand, S., and Bayer, E. M. 2015. Specific membrane lipid composition is important for plasmodesmata function in *Arabidopsis*. Plant Cell 27:1228-1250.

Heinlein, M., and Epel, B. L. 2004. Macromolecular transport and signaling through plasmodesmata. Int. Rev. Cytol. 235:93-164.

Hellemans, J., Mortier, G., De Paepe, A., Speleman, F., and Vandesompele, J. 2007. qBase relative quantification framework and software for management and automated analysis of real-time quantitative PCR data. Genome Biol. 8:R19.

Holdaway-Clarke, T. L., Walker, N. A., Hepler, P. K., and Overall, R. L. 2000. Physiological elevations in cytoplasmic free calcium by cold or ion injection result in transient closure of higher plant plasmodesmata. Planta 210:329-335.

Johnston, M. G., and Faulkner, C. 2021. A bootstrap approach is a superior statistical method for the comparison of non-normal data with differing variances. New Phytol. 230:23-26.

Kankanala, P., Czymmek, K., and Valent, B. 2007. Roles for rice membrane dynamics and plasmodesmata during biotrophic invasion by the blast fungus. Plant Cell 19:706-724.

Khang, C. H., Berruyer, R., Giraldo, M. C., Kankanala, P., Park, S.-Y., Czymmek, K., Kang, S., and Valent, B. 2010. Translocation of *Magnaporthe oryzae* effectors into rice cells and their subsequent cell-to-cell movement. Plant Cell 22:1388-1403.

Kim, J. Y., Yuan, Z., Cilia, M., Khalfan-Jagani, Z., and Jackson, D. 2002. Intercellular trafficking of a *KNOTTED1* green fluorescent protein fusion in the leaf and shoot meristem of *Arabidopsis*. Proc. Natl. Acad. Sci. U.S.A. 99:4103-4108.

Kragler, F., Monzer, J., Shash, K., Xoconostle-Cázares, B., and Lucas, W. J. 1998. Cell-to-cell transport of proteins: Requirement for unfolding and characterization of binding to a putative plasmodesmal receptor. Plant J. 15:367-381.

Kuznetsova, I., Lugmayr, A., Siira, S. J., Rackham, O., and Filipovska, A. 2019. CirGO: An alternative circular way of visualising gene ontology terms. BMC Bioinf. 20:84.

Lee, J.-Y., Wang, X., Cui, W., Sager, R., Modla, S., Czymmek, K., Zybaliov, B., van Wijk, K., Zhang, C., Lu, H., and Lakshmanan, V. 2011. A plasmodesmata-localized protein mediates crosstalk between cell-to-cell communication and innate immunity in *Arabidopsis*. Plant Cell 23:3353-3373.

Le Fevre, R., Evangelisti, E., Rey, T., and Schornack, S. 2015. Modulation of host cell biology by plant pathogenic microbes. Annu. Rev. Cell Dev. Biol. 31:201-229.

Li, H., Handsaker, B., Wysoker, A., Fennell, T., Ruan, J., Homer, N., Marth, G., Abecasis, G., Durbin, R., and 1000 Genome Project Data Processing Subgroup. 2009. The sequence alignment/map format and SAM tools. Bioinformatics 25:2078-2079.

Li, Z., Variz, H., Chen, Y., Liu, S.-L., and Aung, K. 2021. Plasmodesmata-dependent intercellular movement of bacterial effectors. Front Plant Sci. 12:640277.

Liu, L., and Chen, X. 2018. Intercellular and systemic trafficking of RNAs in plants. Nat. Plants 4:869-878.

Lo Presti, L., Lanver, D., Schweizer, G., Tanaka, S., Liang, L., Tollot, M., Zuccaro, A., Reissmann, S., and Kahmann, R. 2015. Fungal effectors and plant susceptibility. Annu. Rev. Plant Biol. 66:513-545.

Love, M. I., Huber, W., and Anders, S. 2014. Moderated estimation of fold change and dispersion for RNA-seq data with DESeq2. Genome Biol. 15:550.

O'Connell, R. J., Thon, M. R., Hacquard, S., Amyotte, S. G., Kleemann, J., Torres, M. F., Damm, U., Buiate, E. A., Epstein, L., Alkan, N., Altmüller, J., Alvarado-Balderrama, L., Bauser, C. A., Becker, C., Birren, B. W., Chen, Z., Choi, J., Crouch, J. A., Duvick, J. P., Farman, M. A., Gan, P., Heiman, D., Henrissat, B., Howard, R. J., Kabbage, M., Koch, C., Kracher, B., Kubo, Y., Law, A. D., Lebrun, M.-H., Lee, Y.-H., Miyara, I., Moore, N., Neumann, U., Nordström, K., Panaccione, D. G., Panstruga, R., Place, M., Proctor, R. H., Prusky, D., Rech, G., Reinhardt, R., Rollins, J. A., Rounsley, S., Schardl, C. L., Schwartz, D. C., Shenoy, N., Shirasu, K., Sikhakolli, U. R., Stüber, K., Sukno, S. A., Sweigard, J. A., Takano, Y., Takahara, H., Trail, F., van der Does, H. C., Voll, L. M., Will, I., Young, S., Zeng, Q., Zhang, J., Zhou, S., Dickman, M. B., Schulze-Lefert, P., Ver Loren van Themaat, E., Ma, L.-J., and Vaillancourt, L. J. 2012. Lifestyle transitions in plant pathogenic *Colletotrichum* fungi deciphered by genome and transcriptome analyses. Nat. Genet. 44: 1060-1065.

Oparka, K. J., Roberts, A. G., Boevink, P., Cruz, S. S., Roberts, I., Pradel, K. S., Imlau, A., Kotlizky, G., Sauer, N., and Epel, B. 1999. Simple, but not branched, plasmodesmata allow the nonspecific trafficking of proteins in developing tobacco leaves. Cell 97:743-754.

R Core Team. 2020. R: A language and environment for statistical computing, v4.0.3. R Foundation for Statistical Computing, Vienna. https://www.R-project.org

Reyes Caldas, P. A., Zhu, J., Breakspear, A., Thapa, S. P., Toruño, T. Y., Perilla-Henao, L. M., Casteel, C., Faulkner, C. R., and Coaker, G. 2022. Effectors from a bacterial vector-borne pathogen exhibit diverse subcellular localisation, expression profiles, and manipulation of plant defense. Mol. Plant-Microbe Interact. 35:1067-1080.

Rutschow, H. L., Baskin, T. I., and Kramer, E. M. 2011. Regulation of solute flux through plasmodesmata in the root meristem. Plant Physiol. 155:1817-1826.

Schindelin, J., Arganda-Carreras, I., Frise, E., Kaynig, V., Longair, M., Pietzsch, T., Preibisch, S., Rueden, C., Saalfeld, S., Schmid, B., Tinevez, J.-Y., White, D. J., Hartenstein, V., Eliceiri, K., Tomancak, P., and Cardona, A. 2012. Fiji: An open-source platform for biological-image analysis. Nat. Methods 9:676-682.

Stahl, Y., and Simon, R. 2013. Gated communities: Apoplastic and symplastic signals converge at plasmodesmata to control cell fates. J. Exp. Bot. 64:5237-5241.

Taoka, K.-i., Ham, B.-K., Xoconostle-Cázares, B., Rojas, M. R., and Lucas, W. J. 2007. Reciprocal phosphorylation and glycosylation recognition motifs control NCAPP1 interaction with pumpkin phloem proteins and their cell-to-cell movement. Plant Cell 19:1866-1884.

Tee, E. E., Samwald, S., and Faulkner, C. 2022. Quantification of cell-to-cell connectivity using particle bombardment. Pages 263-272 in: Plasmodesmata, 2nd ed. Y. Benitez-Alfonso and M. Heinlein, eds. Methods in Molecular Biology, 2457. Humana, New York.

Tomczynska, I., Stumpe, M., Doan, T. G., and Mauch, F. 2020. A *Phytophthora* effector protein promotes symplastic cell-to-cell trafficking by physical interaction with plasmodesmata-localised callose synthases. New Phytol. 227:1467-1478.

Toruño, T. Y., Stergiopoulos, I., and Coaker, G. 2016. Plant-pathogen effectors: Cellular probes interfering with plant defenses in spatial and temporal manners. Annu. Rev. Phytopathol. 54:419-441.

Ueki, S., and Citovsky, V. 2005. Identification of an interactor of cadmium ion-induced glycine-rich protein involved in regulation of callose levels in plant vasculature. Proc. Natl. Acad. Sci. U.S.A. 102:12089-12094.

Wu, X., Dinneny, J. R., Crawford, K. M., Rhee, Y., Citovsky, V., Zambryski, P. C., and Weigel, D. 2003. Modes of intercellular transcription factor movement in the *Arabidopsis* apex. Development 130:3735-3745.

Xu, B., Cheval, C., Laohavisit, A., Hocking, B., Chiasson, D., Olsson, T. S. G., Shirasu, K., Faulkner, C., and Gilliham, M. 2017. A calmodulin-like protein regulates plasmodesmal closure during bacterial immune responses. New Phytol. 215:77-84.

Xu, X. M., Wang, J., Xuan, Z., Goldshmidt, A., Borrill, P. G. M., Hariharan, N., Kim, J. Y., and Jackson, D. 2011. Chaperonins facilitate KNOTTED1 cell-to-cell trafficking and stem cell function. Science 333:1141-1144.

Yan, Y., Ham, B.-K., Chong, Y. H., Yeh, S.-D., and Lucas, W. J. 2020. A plant SMALL RNA-BINDING PROTEIN 1 family mediates cell-to-cell trafficking of RNAi signals. Mol. Plant 13:321-335.